

High-pressure Raman spectroscopic studies of hydrous wadsleyite II

ANNETTE K. KLEPPE,^{1,*} ANDREW P. JEPHCOAT,^{1,2} AND JOSEPH R. SMYTH³

¹Department of Earth Sciences, University of Oxford, Parks Road, Oxford, OX1 3PR, U.K.

²Diamond Light Source, Chilton, Didcot, Oxfordshire, OX11 0QX, U.K.

³Department of Geological Sciences, University of Colorado, Boulder, Colorado 80309, U.S.A.

ABSTRACT

Raman spectra in the range 80 to 4000 cm^{-1} of wadsleyite II (Fo_{90} with 2.0 wt% H_2O and Fo_{88} with 2.7 wt% H_2O) have been measured in a diamond-anvil cell with solid rare-gas pressure-transmitting media to 51.4 GPa at room temperature. The ambient Raman spectrum of wadsleyite II is closely similar to wadsleyite modified with bands in frequency regions where the SiO_4 tetrahedral and OH stretching vibrations of hydrous ringwoodite occur. The most intense, characteristic wadsleyite II modes at 709 and 911 cm^{-1} (Si_2O_7 and SiO_3 symmetric stretching vibrations, respectively) shift continuously to 51.4 GPa showing no evidence for a change in the crystal structure. A striking feature in the high-pressure Raman spectra of wadsleyite II is a significant growth in intensity in the mid-frequency range (300–650 cm^{-1} at 10⁻⁴ GPa and 400–750 cm^{-1} at 51.4 GPa) under compression accompanied by the appearance of new Raman modes near 40 GPa, perhaps a result of resonance electronic Raman scattering. In the OH stretching frequency range, the Raman spectrum of wadsleyite II exhibits at least six modes and their high-pressure behavior agrees with that of Fo_{90} hydrous wadsleyite: OH stretching modes above 3530 cm^{-1} remain approximately constant up to at least 21.8 GPa whereas OH modes at frequencies <3530 cm^{-1} decrease with increasing pressure. The OH stretching modes are consistent with protonation of the non-silicate oxygen O2 and the O atoms surrounding the partially vacant tetrahedral site Si2, as suggested from X-ray diffraction data.

Keywords: Hydrous wadsleyite II, Raman spectroscopy, diamond-anvil cell, transition zone, high pressure

INTRODUCTION

In the system $\text{MgO-FeO-SiO}_2\text{-H}_2\text{O}$ the transformation from olivine [$\alpha\text{-(Mg,Fe)}_2\text{SiO}_4$] to ringwoodite [$\gamma\text{-(Mg,Fe)}_2\text{SiO}_4$, spinel] can involve intermediate phases, the spinelloids (spinel derivatives) wadsleyite [$\beta\text{-(Mg,Fe)}_2\text{SiO}_4$] and wadsleyite II. Wadsleyite II is a hydrous magnesium-iron silicate with variable composition that occurs between the stability regions of wadsleyite and ringwoodite, if sufficient trivalent cations (Fe^{3+} , Al^{3+}) are available (Smyth et al. 2005). It is a possible transition zone phase that is a potential host for hydrogen in the Earth's interior. If present in the transition zone, wadsleyite II may account for the generally diffuse nature and splitting of the 520 km seismic discontinuity observed in some regions of the Earth's mantle (Smyth et al. 2005). Smyth and Kawamoto (1997) were the first to report the synthesis and full three-dimensional crystal structure of wadsleyite II. Recently, Smyth et al. (2005) characterized the wadsleyite II phase in further detail using different techniques including electron microscopy, high-pressure single-crystal X-ray diffraction, and Fourier transform infrared (FTIR), Raman, and Mössbauer spectroscopy.

The crystal structure of wadsleyite II (Fig. 1) belongs to the orthorhombic crystal system, space group *Imma*. The unit-cell parameters are $a = 5.6884(4)$ Å, $b = 28.9238(15)$ Å, and $c = 8.2382(6)$ Å; a and c are approximately the cell parameters of

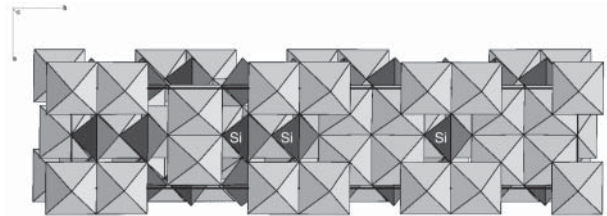


FIGURE 1. The crystal structure of wadsleyite II.

wadsleyite whereas b is 2.5 times that of wadsleyite (Smyth and Kawamoto 1997; Smyth et al. 2005). Unlike the olivine and spinel crystal structures that contain only isolated SiO_4 tetrahedra, the wadsleyite structures contain polymerized tetrahedra: in wadsleyite solely Si_2O_7 groups are present, whereas in wadsleyite II both single (SiO_4) and coupled tetrahedra (Si_2O_7) exist: one-fifth of the Si atoms is in isolated tetrahedra and four-fifths in Si_2O_7 groups so that the structure can be thought of as a mixture of one-fifth spinel and four-fifths wadsleyite.

The wadsleyite II structure contains three distinct tetrahedral sites (Si1–Si3), six different (Mg,Fe) octahedral sites (M1–M6), and eight distinct oxygen sites (O1–O8) Si1 is an isolated SiO_4 group, and Si2 and Si3 form an Si_2O_7 group. O7 is the bridging O atom of the Si_2O_7 group and also bonded to one M3; the O2 atom is not bonded to Si, but is coordinated by five M site atoms, two M5, two M6, and one M3 (Smyth et al. 2005). The other O atoms are each bonded to three M and one Si, and are similar

* E-mail: annette.kleppe@earth.ox.ac.uk

to the oxygen sites in olivine and ringwoodite. The hydration mechanism of wadsleyite II appears to be protonation of the non-silicate oxygen O2 and possibly the O atoms surrounding the partially vacant tetrahedral site Si2. Charge-balance is achieved by cation vacancies in M5, M6, and Si2 (Smyth et al. 2005). Octahedral site vacancy has also been shown to be the principal hydration mechanism in hydrous wadsleyite and hydrous ringwoodite (e.g., Smyth 1994; Smyth et al. 2003).

Ambient Raman spectra of wadsleyite II were reported in the context of phase identification and characterization by Smyth et al. (2005), but the vibrational behavior of wadsleyite II at high pressures has not yet been investigated. Here we report high-pressure Raman spectra in the region from 80 to 4000 cm^{-1} on high-quality single crystals of wadsleyite II measured in a diamond-anvil cell with solid rare-gas pressure-transmitting media to pressures of 51.4 GPa. Our motivation was to track changes in H bonding and proton environments under pressure and to probe for pressure-induced structural changes using a local structural probe. A comparison of the ambient and high-pressure Raman spectroscopic behavior of wadsleyite II with hydrous wadsleyite and hydrous ringwoodite shows the intermediate nature of wadsleyite II with respect to these two phases.

EXPERIMENTAL METHODS

Raman spectroscopic studies were performed on high-quality single crystals of wadsleyite II at ambient conditions and at high pressures up to 51.4 GPa at 300 K. The two wadsleyite II samples used in the present studies were synthesized in a multi-anvil press at 17.5–18 GPa and $\sim 1400^\circ\text{C}$ with a heating time of 18–22 h and subsequently characterized by single-crystal X-ray diffraction, FTIR, Raman, and Mössbauer spectroscopy, electron microprobe (EMP), secondary ion mass spectrometry (SIMS), and transmission electron microscopy (TEM), including electron energy-loss spectroscopy (Smyth and Kawamoto 1997; Smyth et al. 2005). In particular, the major element composition of the crystals was obtained from EMP analysis and the H concentration was extracted from the FTIR (details in Smyth et al. 2005) and SIMS (details in Smyth and Kawamoto 1997). The compositions of samples 1 and 2 are approximately Fo_{90} and Fo_{88} with 2.03(6) and 2.72(24) wt% H_2O (chemical formulae: $\text{Mg}_{1.71}\text{Fe}_{0.18}\text{Al}_{0.01}\text{H}_{0.33}\text{Si}_{0.96}\text{O}_4$ and $\text{Mg}_{1.60}\text{Fe}_{0.22}\text{Al}_{0.01}\text{H}_{0.44}\text{Si}_{0.97}\text{O}_4$), respectively. TEM analysis showed that the crystal lattice of both samples is free of stacking faults, dislocations and hydrous precipitates (Smyth et al. 2005).

Ambient Raman spectra were measured in the range 80–4000 cm^{-1} from single crystal fragments of samples 1 and 2, and also from a coarse powder of sample 1. The powder was prepared by crushing a crystal fragment between two diamond-anvil tips. As the relative intensities of Raman modes do change with changing crystal vs. laser beam orientation, unpolarized Raman spectra were collected in various, arbitrary orientations of the crystals relative to the incident laser beam in this study to observe and reveal as many of the wadsleyite II Raman modes as possible. Ambient Raman spectra of sample 1 were included in Smyth et al. (2005).

Two high-pressure micro-Raman spectroscopic experiments were performed on wadsleyite II. In the first high-pressure run a $\sim 10\ \mu\text{m}$ thick single crystal fragment with flat surfaces of sample 1, about $25 \times 10\ \mu\text{m}$ in size, was mounted in a diamond-anvil cell together with a $<10\ \mu\text{m}$ diameter ruby sphere for pressure calibration (Mao et al. 1978). Fluid helium was loaded at 0.2 GPa (Jephcoat et al. 1987) as a pressure-transmitting medium to ensure hydrostatic conditions. A stainless steel gasket preindented to $25\ \mu\text{m}$ with an $80\ \mu\text{m}$ drilled hole and culets of $300\ \mu\text{m}$ diameter formed the sample chamber. In this first compression experiment the Raman active OH stretching frequencies could not be observed unambiguously above the fluorescence background of the natural, low-fluorescence diamond-anvils. To reduce the fluorescence from the anvils and observe OH stretching modes under compression, we performed a second high-pressure experiment using a diamond-anvil cell equipped with ultra-low fluorescence, synthetic type IIa diamonds (Sumitomo Electric Company) with a culet size of $600\ \mu\text{m}$ in diameter. In this second run a $20\ \mu\text{m}$ thick single crystal fragment of sample 2, about $35 \times 35\ \mu\text{m}$ in size, was loaded in the diamond-anvil cell together with a $<10\ \mu\text{m}$ diameter ruby sphere for pressure calibration and a helium-argon mix as a pressure-transmitting medium. A stainless steel gasket preindented to $50\ \mu\text{m}$ with a $150\ \mu\text{m}$ drilled hole was used.

Unpolarized Raman spectra to 51.4 GPa (first run) and 21.8 GPa (second run) were measured in 135° scattering geometry with a SPEX Triplemate equipped with a back-illuminated liquid- N_2 -cooled CCD detector in the range 30 to 4000 cm^{-1} . This spectral range encompasses both silicate stretching and bending modes, more complicated MgO_6 vibrations and OH stretching and bending frequencies. Data were recorded for both increasing and decreasing pressure. The spectra were excited by the 514.5 and 488 nm line of an argon-ion laser focused to a $5\ \mu\text{m}$ spot on the sample and collected through a confocal aperture giving high spatial resolution at the sample. The intrinsic resolution of the spectrometer is $1.5\ \text{cm}^{-1}$ and calibrations are accurate to $\pm 1\ \text{cm}^{-1}$. Low laser power was required to avoid heating of the dark green wadsleyite II crystals, and hence only long collection times led to an acceptable signal-to-noise ratio. The frequency of each Raman band was obtained by fitting Voigt lineshape functions to the spectra using a least-squares algorithm.

RESULTS

Raman frequencies of wadsleyite II at ambient conditions

The ambient, unpolarized Raman spectrum of wadsleyite II closely resembles at first glance the Raman spectrum of Fo_{90} hydrous wadsleyite in the range 30–1200 cm^{-1} (Fig. 2). It is characterized by two intense modes at 709 and 911 cm^{-1} , which, by analogy with hydrous wadsleyite, are assumed to correspond to the Si_2O_7 symmetric stretching vibration (Si-O-Si of the disilicate group) and the symmetric stretching vibration of the SiO_3 terminal unit, respectively. However, there are subtle differences between the Raman spectra of wadsleyite II and Fo_{90} hydrous wadsleyite: (1) the frequencies of the Si_2O_7 and SiO_3 symmetric stretching vibrations of wadsleyite II are clearly lower than those of hydrous wadsleyite (Table 1); (2) in the wadsleyite II spectrum the 709 cm^{-1} mode appears asymmetric with a shoulder on its low frequency side; and (3) the 911 cm^{-1} mode exhibits high, distinct shoulders on both sides with a relatively intense mode being resolved at 773 cm^{-1} in the spectrum of the wadsleyite II powder sample (Fig. 2a). The 773 cm^{-1} mode occurs close to the frequency range of the characteristic SiO_4 tetrahedral stretching vibrations of Fo_{89} hydrous ringwoodite (Fig. 2d) (Kleppe et al. 2002b). Hence the Raman spectrum of the wadsleyite II powder sample looks like a superposition of a Fe-bearing hydrous wadsleyite and ringwoodite spectrum.

This superposed appearance of the wadsleyite II spectrum holds also true for the OH stretching frequency range (Fig. 3): between 3350 and 3600 cm^{-1} the wadsleyite II spectrum shows modes similar to those of Fo_{90} hydrous wadsleyite, but overlain with the broad OH stretching bands of ringwoodite that occur at 3165 and 3685 cm^{-1} (full width at half maximum around 350 and 150–200 cm^{-1} respectively, Kudoh et al. 2000). The spectrum of the OH stretching modes of sample 1 can be fitted with a minimum of six bands (Fig. 4); only five bands are resolved in the weaker spectrum of sample 2 (Table 1). The Raman spectra in the OH stretching frequency range of wadsleyite II are in overall agreement with the IR spectra (Smyth et al. 2005).

Pressure dependence of the framework Raman modes of wadsleyite II

High-frequency range: 650–1300 cm^{-1} . Representative Raman spectra in the region 30–1300 cm^{-1} of samples 1 and 2 of wadsleyite II as a function of pressure are shown in Figures 5 and 6, respectively. The pressure dependence of each mode is shown in Figure 7. The characteristic wadsleyite II modes at 709 and 911 cm^{-1} (Si_2O_7 and SiO_3 symmetric stretching vibrations, respectively) shift continuously up to the highest pressure of

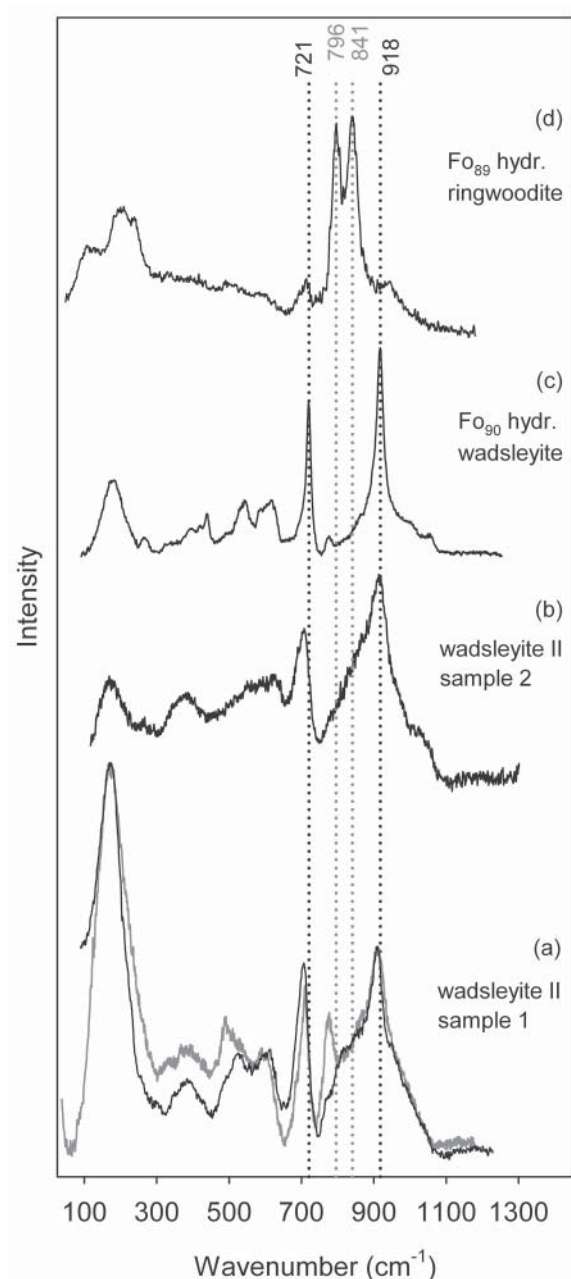


FIGURE 2. Ambient Raman spectra in the range 30 to 1300 cm^{-1} of (a) wadsleyite II sample 1 (black = single-crystal fragment; gray = powder; Smyth et al. 2005) and (b) wadsleyite II sample 2 (present study). For comparison Raman spectra of (c) Fo_{90} hydrous wadsleyite with 2.4 wt% H_2O (Kleppe et al. 2006), and (d) Fo_{89} hydrous ringwoodite with 1.6 wt% H_2O (Kleppe et al. 2002b) are shown. The relative mode intensities depend on the orientation of the crystal relative to the incident laser beam. Black dotted lines represent characteristic and intense modes of the wadsleyite structure: Si_2O_7 symmetric stretching vibration at 721 cm^{-1} and symmetric stretching vibration of the SiO_3 terminal unit at 918 cm^{-1} . Gray dotted lines correspond to the most intense, characteristic spinel modes, the antisymmetric (796 cm^{-1}) and symmetric (841 cm^{-1}) stretching vibrations of the SiO_4 tetrahedra.

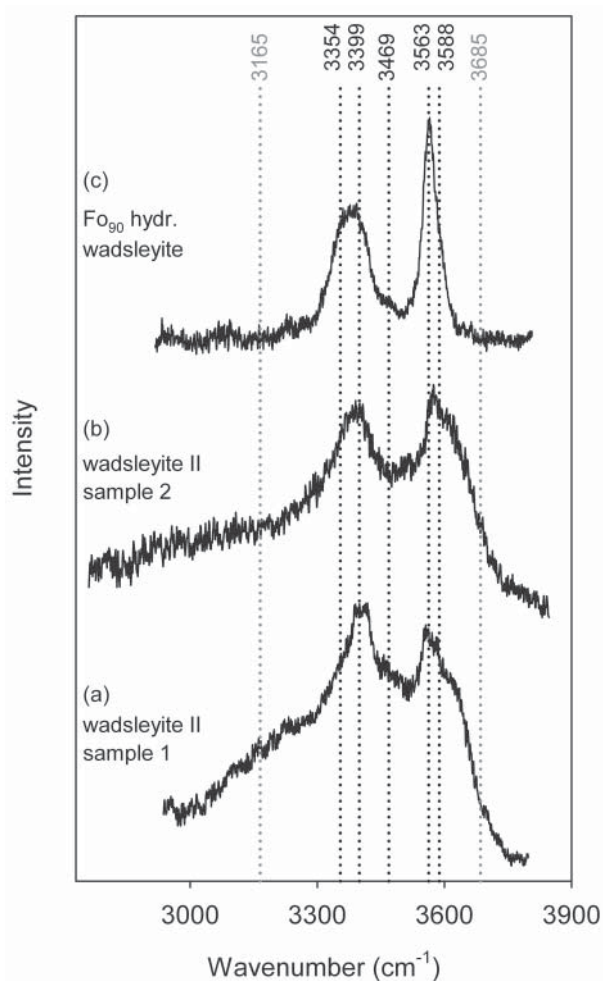


FIGURE 3. Comparative, ambient Raman spectra in the OH stretching frequency region of (a) wadsleyite II sample 1 (Smyth et al. 2005), (b) wadsleyite II sample 2 (present study), and (c) Fo_{90} hydrous wadsleyite with 2.4 wt% H_2O (Kleppe et al. 2006). The relative mode intensities depend on the orientation of the crystal relative to the incident laser beam. Black dotted lines show the OH stretching frequencies of Fo_{90} hydrous wadsleyite, and gray dotted lines represent the position of the OH stretching frequencies of Fo_{100} hydrous ringwoodite (Kudoh et al. 2000).

51.4 GPa giving no indication for a first-order crystal structural change. The pressure dependence of the 911 cm^{-1} mode agrees within error with the pressure dependence of the 918 cm^{-1} mode of Fo_{90} hydrous wadsleyite, whereas the pressure dependence of the 709 cm^{-1} mode of wadsleyite II is rather intermediate between the pressure dependence of the 721 cm^{-1} mode of Fo_{90} hydrous wadsleyite and the 709 cm^{-1} mode of Fo_{89} hydrous ringwoodite. The ambient 773 cm^{-1} mode of wadsleyite II, thought to be associated with stretching vibrations of the SiO_4 tetrahedra, was not resolved as a distinct peak under pressure. The pressure dependence of the SiO_4 stretching modes of ringwoodite lie within the range of the pressure dependence of the two to three shoulders observed on the low-frequency side of the 911 cm^{-1} mode (Fig. 7).

TABLE 1. Comparison of the mode frequencies and pressure derivatives of wadsleyite II with Fo₉₀ and Fo₁₀₀ hydrous wadsleyite

Wadsleyite II (sample 1, Fo ₉₀ , 2.0 wt% H ₂ O, present study) to 51.4 GPa		Wadsleyite II (sample 2, Fo ₉₀ , 2.7 wt% H ₂ O, present study) to 21.8 GPa		Fo ₉₀ hydrous wadsleyite (2.4 wt% H ₂ O, Kleppe et al. 2006) to 58.4 GPa		Fo ₁₀₀ hydrous wadsleyite (1.65 wt% H ₂ O, Kleppe et al. 2001) to 50 GPa	
ν (cm ⁻¹)	$\partial\nu/\partial P$ (cm ⁻¹ /GPa)	ν (cm ⁻¹)	$\partial\nu/\partial P$ (cm ⁻¹ /GPa)	ν (cm ⁻¹)	$\partial\nu/\partial P$ (cm ⁻¹ /GPa)	ν (cm ⁻¹)	$\partial\nu/\partial P$ (cm ⁻¹ /GPa)
171		172		179			
246*		250*		267		229	
*		*		†		266	
*		*		†		313	
392*		380*		398		363	
*		*				406	
*		*		420		422	
*		*		440		441	
*		477*				487	
490*		*		492			
*		*		523			
539*		545*		543		549	
*		*		588		588	
604*		624*		619		618	2.04
631§	3.238‡	631§	3.238‡	625§	3.471		
686		685		702			
709	4.340x - 0.0188x ² ‡	709	4.340x - 0.0188x ² ‡	721	3.263x - 0.0051x ²	722	3.368x - 0.0074x ²
773		777		777	4.870x - 0.0163x ²	779	5.055x - 0.0208x ²
811		813					
				840			
864		868		882	4.307x - 0.0176x ²	885	4.328x - 0.0175x ²
911	3.981x - 0.0105x ² ‡	914	3.981x - 0.0105x ² ‡	918	3.263x - 0.0051x ²	916	3.368x - 0.0074x ²
956		965		955			
997				993		978	
1034		1032		1045		1028	
3243		3254	-8.9				
3351				3354		3329	-7.7
3408		3390	-7.4	3399		3373	-7.0
3484		3504	-4.6	3469			
3564		3570	0.1	3563			
				3588		3586	-0.29#
3628		3626	0.7				

Notes: Modes that have been observed over the full pressure range to 51.4 GPa have been fitted with a quadratic term; modes observed only over parts of the investigated pressure range have been assumed to vary linearly.

* This spectral range is characterized by broad features. The minimum number of bands that can be fitted to this part of the spectrum is given.

† Intensity is observed, but modes are not resolved.

‡ Includes data of sample 1 and 2.

§ Extrapolated to 10⁻⁴ GPa.

|| To 10.13 GPa.

To 24 GPa; from 24 to 50 GPa $\partial\nu/\partial P$ is -3.90 (cm⁻¹/GPa).

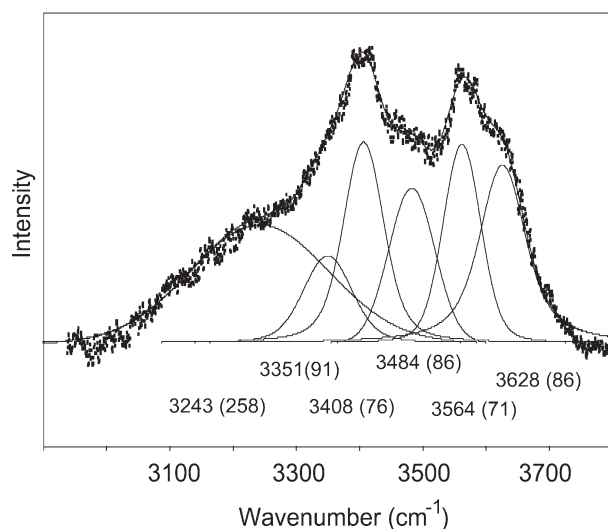


FIGURE 4. Ambient Raman spectrum of the OH stretching modes of wadsleyite II sample 1. Fitted peak positions and in parentheses the respective full width at half maximum are given.

Mid-frequency range: 300–650 cm⁻¹. A striking increase in relative intensity occurs in the Raman spectra of sample 1 in the mid-frequency range (300–650 cm⁻¹ at 10⁻⁴ GPa shifted to 400–750 cm⁻¹ at 51.4 GPa) under compression. A single, broad band that spans the full mid-frequency range at low pressures gains in intensity under compression and at 35 GPa is more intense than the Si₂O₇ and SiO₃ symmetric stretching mode. Above 35 GPa three main modes emerge out of the broad band gaining further in intensity to the highest pressure of this study. Extrapolation down to 10⁻⁴ GPa shows that the modes (508, 353, and 326 cm⁻¹) lie within a range of possible frequencies for wadsleyite II. However, the modes observed above 35 GPa do not correlate with ambient Raman modes of wadsleyite II and hence appear to be new, pressure-induced modes.

The high-pressure evolution of the Raman spectra of wadsleyite II sample 2 (Fig. 6) differs from that of sample 1. The ambient bands in the mid-frequency range do not merge into one single broad band under compression and also a pressure-induced intensity enhancement is absent up to the highest pressure of 21.8 GPa. Differences between the Raman spectra of the two wadsleyite II samples are likely due to the slightly different

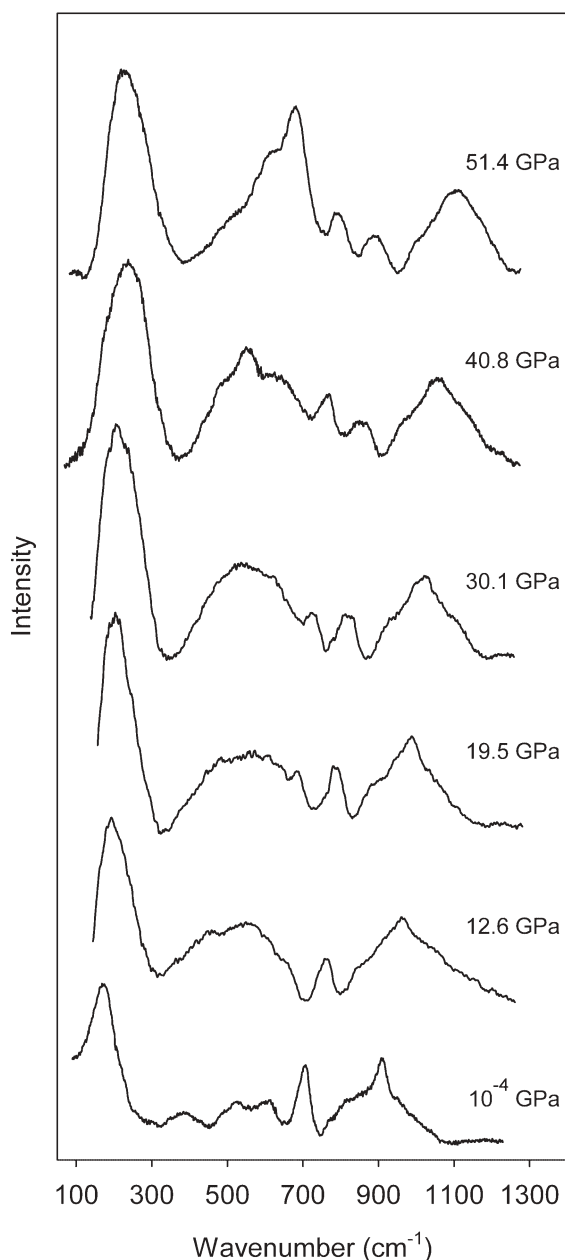


FIGURE 5. Selected Raman spectra of wadsleyite II sample 1 as a function of pressure in the wavenumber range 50–1300 cm^{-1} .

synthesis conditions (P , T) of the two samples, intrinsic sample differences (composition), and differences in the probed surfaces of the single-crystal fragments. The observed, pressure-induced changes in the Raman spectra of wadsleyite II sample 1 are reversible without hysteresis and are not generated or affected by non-hydrostatic stresses in the sample because we used helium as pressure-transmitting medium, and neither the ruby nor the silicate stretching modes gave any evidence for a significant pressure gradient across the sample.

Low-frequency range: 30–300 cm^{-1} . A relatively intense feature in the Raman spectra of wadsleyite II occurs at low

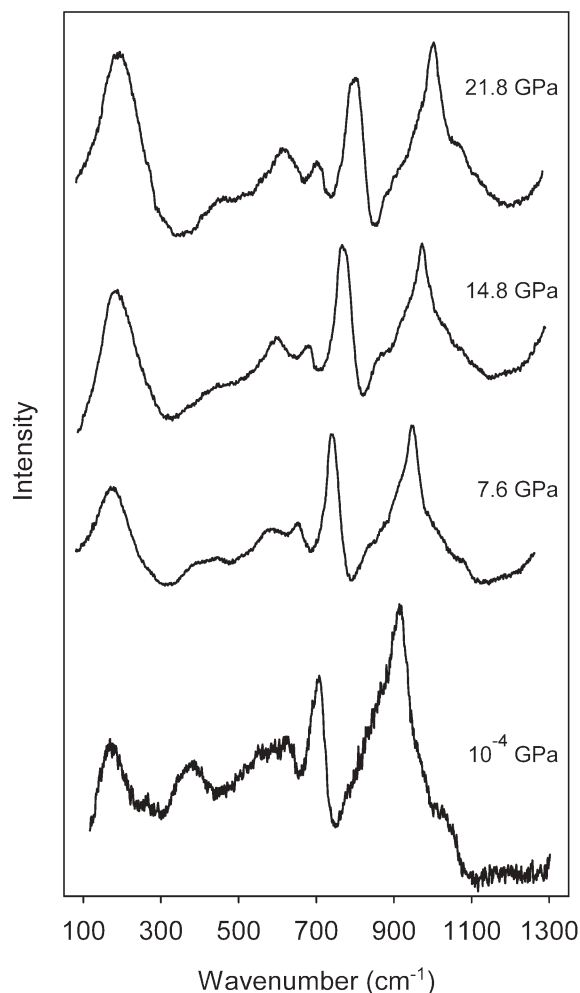


FIGURE 6. Selected Raman spectra of wadsleyite II sample 2 as a function of pressure in the wavenumber range 50–1300 cm^{-1} .

frequencies centered around 171 cm^{-1} at 10^{-4} GPa. Its pressure dependence is relatively weak, but it gains in intensity relative to characteristic wadsleyite II modes under compression. Part of the intensity increase appears to be retained on decompression indicating an irreversible modification in the crystal structure. This observation is similar to our observation in the Raman spectra of Fo_{90} hydrous wadsleyite (Kleppe et al. 2006) where the low-frequency feature was suggested to be associated with localized modes generated by the presence of Fe (Fe^{2+} , Fe^{3+}) in the hydrous wadsleyite structure. The pressure-induced intensity increase might be connected to energetically favored site distortions under compression. Additional work is required to understand this low-frequency feature and any possible correlation with local disorder in the structure.

Pressure dependence of the OH stretching modes of wadsleyite II

Figure 8 shows representative Raman spectra of wadsleyite II sample 2 as a function of pressure in the OH stretching region to 21.8 GPa, the highest pressure of the experiment on sample 2. The OH stretching modes broaden and weaken under compression,

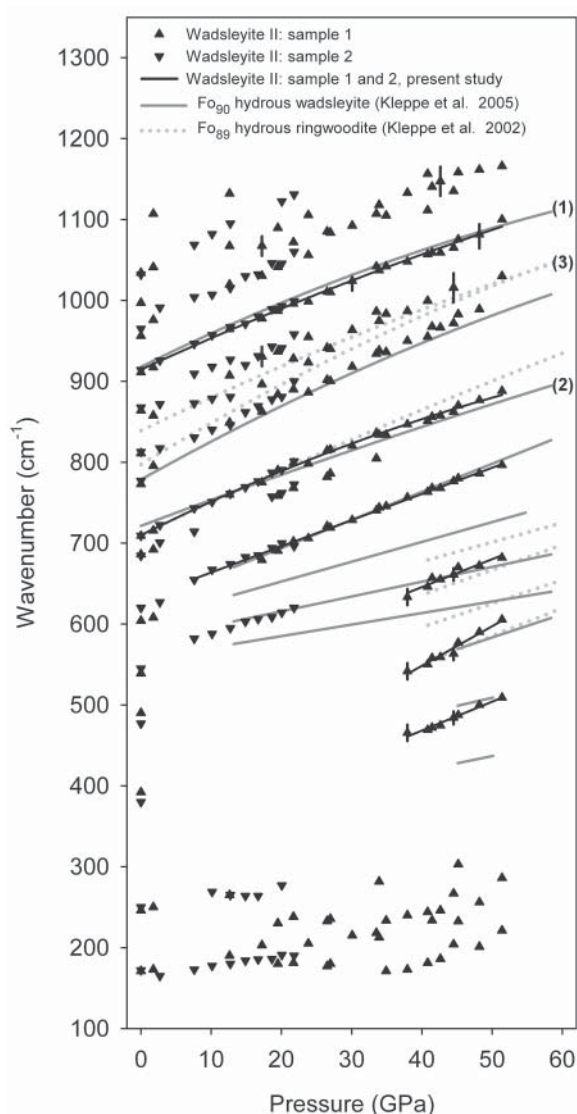


FIGURE 7. Pressure dependence of the framework Raman modes of wadsleyite II. The error in measurement of both frequency and pressure is within the size of the symbol except where representative error bars are given. Modes observed over the entire pressure range have been fitted with a quadratic term; modes that could only be located reliably over parts of the investigated pressure range have been assumed to vary linearly. For comparison the pressure dependence of some framework modes of Fo_{90} hydrous wadsleyite and Fo_{89} hydrous ringwoodite are given. Characteristic wadsleyite modes are: (1) Si_2O_7 symmetric stretching vibration (Si-O-Si of the disilicate group), and (2) symmetric stretching vibration of the SiO_3 terminal unit. Typical modes of ringwoodite are (3) the antisymmetric and symmetric stretching vibrations of the SiO_4 tetrahedra.

in particular the OH modes below 3530 cm^{-1} . The OH doublet at 3570 and 3626 cm^{-1} was resolved up to 13 GPa and was tracked as a single mode at higher pressures. The pressure dependence of the OH Raman modes of wadsleyite II (Fig. 9) contrasts strongly with that of the framework modes OH stretching modes above 3530 cm^{-1} remain approximately constant up to at least 21.8 GPa

whereas OH modes at lower frequencies decrease with increasing pressure; the lower the ambient OH stretching frequency the more negative its pressure dependence (Table 1). The high-pressure behavior of all the OH stretching modes is in accord with previous studies on Fo_{90} hydrous wadsleyite (Kleppe et al. 2006) and Fo_{100} hydrous wadsleyite (Kleppe et al. 2001).

DISCUSSION

Ambient Raman spectra of wadsleyite II in comparison with hydrous wadsleyite and hydrous ringwoodite

Wadsleyite II is intermediate in stability and crystal structural properties between wadsleyite and ringwoodite. Its ambient Raman spectrum reflects the spinelloid structure and exhibits both hydrous wadsleyite and ringwoodite modes compatible with the structural unit model comprising a mixture of four-fifths wadsleyite and one-fifth spinel. The spectrum is dominated by a close similarity to hydrous wadsleyite modified with bands in frequency regions where the SiO_4 tetrahedral and OH stretching vibrations of hydrous ringwoodite occur. The mode structure of wadsleyite II is, in comparison with Fo_{90} hydrous wadsleyite, relatively broad, especially in the mid-frequency range ($300\text{--}650\text{ cm}^{-1}$). Broader modes in wadsleyite II can be associated with increased structural site distortions due to alternating wadsleyite and spinel-type units (Si_2O_7 and SiO_4) in the structure (Horiuchi et al. 1982). Further, the incorporation of Fe, in particular Fe^{3+} , in octahedral sites and hydrogen contributes to the distortion of structural sites and formation of vacancies. The relatively small, but distinct differences between the Raman spectra of wadsleyite II and hydrous wadsleyite confirm that good quality Raman measurements can be used to discriminate between structurally closely related phases.

High-pressure Raman spectra ($30\text{--}1300\text{ cm}^{-1}$) of wadsleyite II in comparison with hydrous wadsleyite and hydrous ringwoodite

The high-pressure evolution of the Raman spectra of wadsleyite II and hydrous wadsleyite is very similar as expected for phases with closely related crystal structures. Both spinelloids remain stable despite compression well beyond pressures in the transition zone at room temperature (51.4 GPa corresponds to about 1300 km depth). There is no indication for a first-order crystal structural change in the pressure dependence of their characteristic Si_2O_7 and SiO_3 symmetric stretching modes. A striking feature in the high-pressure Raman spectra of both wadsleyite II and Fo_{90} hydrous wadsleyite is a significant growth in intensity of bands in the mid-frequency range relative to the Si_2O_7 and SiO_3 symmetric stretching modes under compression accompanied by the appearance of new Raman modes near 40 GPa. Interestingly, a similar observation has been made in the high-pressure Raman spectra of Fo_{89} hydrous ringwoodite (Kleppe et al. 2002b). The difference between the hydrous ringwoodite and hydrous wadsleyite case is that for hydrous ringwoodite the pressure-induced modes appear at frequencies clearly forbidden for the ideal, cubic spinel structure, whereas for hydrous wadsleyite the presence of modes in the mid-frequency-range is not unusual. In contrast to the iron-bearing hydrous spinelloids and spinel, the high-pressure Raman spectra of the hydrous Mg end-member phases do

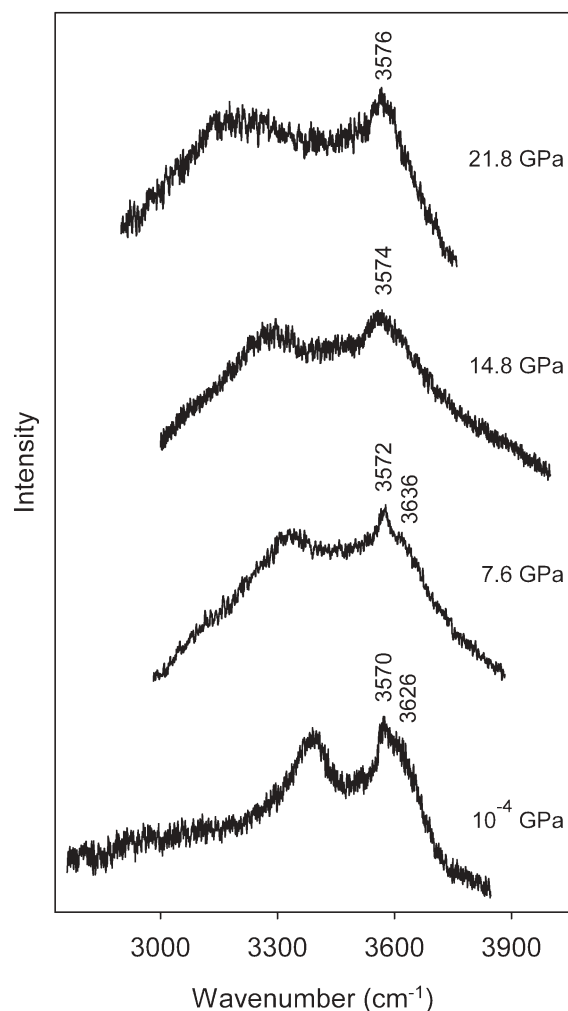


FIGURE 8. Selected Raman spectra of wadsleyite II sample 2 as a function of pressure in the OH stretching frequency region.

not show enhanced intensity and emergence of pressure-induced Raman modes in the mid-frequency range under compression (Kleppe et al. 2001; 2002a). Hence, our observations appear to be connected to Fe (Fe^{2+} , Fe^{3+})-substitution in the hydrous Mg end-member structures. The compositions of the iron-bearing hydrous wadsleyite, wadsleyite II and ringwoodite samples discussed here are close to Fo_{90} with about 30–40, ~55, and ~10% of the total Fe being Fe^{3+} , respectively (Smyth et al. 2005, McCammon et al. 2004).

On resonance electronic Raman scattering in wadsleyite II and ringwoodite

One explanation for the observed, pressure-induced changes in the Raman spectra of iron-containing hydrous wadsleyite, wadsleyite II, and ringwoodite might be resonance electronic Raman scattering. This process can originate from the presence of Fe^{2+} in octahedral sites and can cause striking intensity enhancement together with new modes at frequencies forbidden for vibrational Raman modes. Electronic transitions related to the substitution of Fe^{2+} for Mg^{2+} on octahedral sites have been

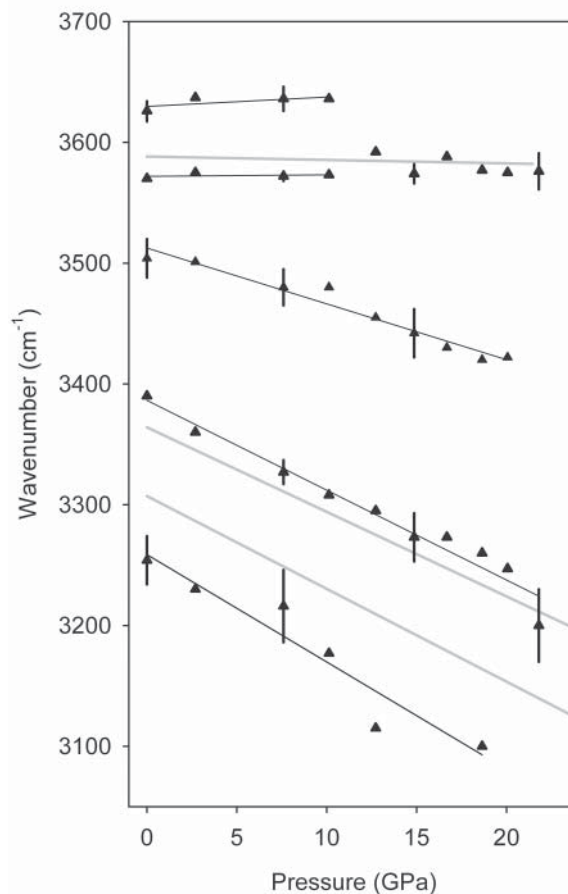


FIGURE 9. Pressure dependence of the OH stretching modes of wadsleyite II sample 2. Representative error bars are given where errors are larger than the size of the symbol. The pressure dependence of the OH modes of Fo_{100} hydrous wadsleyite (gray lines; Kleppe et al. 2001) is given for comparison.

observed in the optical and near infrared absorption spectra of wadsleyite II and ringwoodite (Keppler and Smyth 2005; Smyth et al. 2005). The spectra of ringwoodite are characterized by two absorption bands at 8678 and 12265 cm^{-1} due to spin-allowed crystal-field transitions of octahedral Fe^{2+} (Keppler and Smyth 2005). The pressure dependence of the crystal field bands has been established to 21.5 GPa and is 77.5 $\text{cm}^{-1}/\text{GPa}$ for the dominant, ambient 12265 cm^{-1} crystal-field band (Keppler and Smyth 2005). The full width at half maximum of this band (~5000 cm^{-1}) does not change significantly under pressure. Extrapolation to 40 GPa shifts the dominant crystal-field transition band to 15365 cm^{-1} , and hence near 40 GPa this crystal-field transition band starts to overlap significantly with the 514.5 nm (19436 cm^{-1}) laser excitation line. This overlap facilitates resonance excitation involving crystal-field levels of octahedral Fe^{2+} . The coincidence, and hence resonance, between the laser excitation line and the crystal-field levels improves under further compression causing a discrete, electronic Raman mode structure in the mid-frequency range at higher pressures, which is more intense than the vibrational Raman modes (Fig. 3 in Kleppe et al. 2002b). The fact

that the phonon intensities remain about the same level while the electronic Raman intensities become strongly enhanced indicates that the coupling between the electronic states of Fe^{2+} and the lattice vibrations is very weak.

Similar considerations hold true for wadsleyite II; the optical and near infrared absorption spectrum of wadsleyite II shows a band centered around 10638 cm^{-1} due to crystal field transitions of octahedral Fe^{2+} at 10^{-4} GPa (Smyth et al. 2005). High-pressure absorption spectra do not exist but a shift of the crystal-field band to higher frequencies under compression is expected. Assuming that the band has a pressure-dependence similar to that of the crystal-field transition bands of ringwoodite, we can also explain the intense mode structure in the mid-frequency range above 40 GPa of wadsleyite II in terms of resonant electronic Raman modes. Fluorescence as origin of the modes can be excluded as 488 nm (20492 cm^{-1}) laser excitation results in identical frequencies for all modes. The electronic Raman scattering is present in both, spectra excited with 514.8 and 488 nm, because the difference in the excitation energies is small with respect to the half width of the crystal-field transition bands.

Hydroxyl groups in hydrous wadsleyite II

The ambient Raman spectrum of wadsleyite II consists of at least six OH stretching modes. Assuming linear O-H \cdots O topologies we can correlate the observed OH stretching frequencies with O \cdots O bond distances using the empirical correlation by Libowitzky (1999). The broad and weak OH band at 3243 cm^{-1} corresponds to an O \cdots O distance of about 2.7 Å, the triplet at 3351, 3408, and 3484 cm^{-1} fits with O \cdots O distances around 2.8 Å, and the doublet at 3564 and 3628 cm^{-1} only allows O \cdots O distances ≥ 3 Å. These distances are in overall agreement with protonation of the O atoms surrounding the partially vacant tetrahedral site Si2 (average edge length is about 2.73 Å) and the non-silicate oxygen O2, as suggested from single-crystal X-ray diffraction data (Smyth et al. 2005).

The Raman active OH stretching modes of wadsleyite II with frequencies $<3530\text{ cm}^{-1}$ have a strong, negative pressure dependence whereas OH modes at higher frequencies are less sensitive to pressure with their wavenumbers being approximately constant to at least 21.8 GPa. This is consistent with previous high-pressure Raman studies on Fo_{90} hydrous wadsleyite (Kleppe et al. 2006) and Fo_{100} hydrous wadsleyite (Kleppe et al. 2001). A nearly constant OH stretching frequency under compression suggests very weak hydrogen bonding. A negative frequency response of OH modes under pressure requires a reduction of the respective O \cdots O distances and reflects a strengthening of the hydrogen bond. A concomitant lengthening of the O-H bond has often been assumed but is not mandatory; e.g., Parise et al. (1994) demonstrated that in deuterated brucite the O-D bond length is constant under compression to 9.36 GPa.

Neutron experiments would be best to determine unambiguously the protonation sites in wadsleyite and might become pos-

sible at the high pressures and small sample volumes needed with the higher neutron fluxes available in the future.

ACKNOWLEDGMENTS

This work was supported by Natural Environment Research Council fellowship NER/I/S/2001/00723 and grant NER/B/S/2003/00258 to A.K.K., and Natural Environment Research Council grants GT59801ES, and GR3/10912 to A.P.J. This research was also supported by the U.S. National Science Foundation grant EAR 03-36611 to J.R.S., the Bayerisches Geoinstitut Visitor Program, and the Alexander von Humboldt Foundation. We thank A. Chopelas, E. Libowitzky, and an anonymous reviewer for helpful comments.

REFERENCES CITED

- Horiuchi, H., Akaogi, M., and Sawamoto, H. (1982) Crystal structure studies on spinel-related phases, spinelloids: implications to olivine-spinel phase transformation and systematics. *Advances in Earth and Planetary Sciences*, 12, 391–403.
- Jephcoat, A.P., Mao, H.K., and Bell, P.M. (1987) Operation of the Megabar Diamond-Anvil Cell. In G.C. Ulmer and H.L. Barnes, Eds., *Hydrothermal Experimental Techniques*, 469 p. Wiley-Interscience, New York.
- Keppeler, H. and Smyth, J.R. (2005) Optical and near infrared spectra of ringwoodite to 21.5 GPa: implications for radiative heat transport in the mantle. *American Mineralogist*, 90, 1209–1212. DOI: 10.2138/am.2005.1908
- Kleppe, A.K., Jephcoat, A.P., Olijnyk, H., Slesinger, A.E., Kohn, S.C., and Wood, B.J. (2001) Raman spectroscopic study of hydrous wadsleyite ($\beta\text{-Mg}_2\text{SiO}_4$) to 50 GPa. *Physics and Chemistry of Minerals*, 28, 232–241.
- Kleppe, A.K., Jephcoat, A.P., and Smyth, J.R. (2002a) Raman spectroscopic study of hydrous $\gamma\text{-Mg}_2\text{SiO}_4$ to 56.5 GPa. *Physics and Chemistry of Minerals*, 29, 473–376. DOI: 10.1007/s00269-002-0255-5
- Kleppe, A.K., Jephcoat, A.P., Smyth, J.R., and Frost, D.J. (2002b) On protons, iron, and the high-pressure behavior of ringwoodite. *Geophysical Research Letters*, 29, 17-1–17-4. DOI: 10.1029/2002GL015276
- Kleppe, A.K., Jephcoat, A.P., and Smyth, J.R. (2006) High-pressure Raman spectroscopic study of Fo_{90} hydrous wadsleyite. *Physics and Chemistry of Minerals*, 32, 700–709. DOI: 10.1007/s00269-005-0048-8
- Kudoh, Y., Kuribayashi, T., Mizobata, H., and Ohtani, E. (2000) Structure and cation disorder of hydrous ringwoodite, $\gamma\text{-Mg}_{1.89}\text{Si}_{0.99}\text{H}_{0.30}\text{O}_4$. *Physics and Chemistry of Minerals*, 27, 474–479.
- Libowitzky, E. (1999) Correlation of O-H stretching frequencies and O-H \cdots O hydrogen bond lengths in minerals. *Monatshefte für Chemie*, 130, 1047–1059.
- Mao, H.K., Bell, P.M., Shaner, J.W., and Steinberg, D.J. (1978) Specific volume measurements of Cu, Mo, Pd, and Ag and calibration of the ruby R1 fluorescence pressure gauge from 0.06 to 1 Mbar. *Journal of Applied Physics*, 49(6), 3276–3283.
- McCammon, C.A., Frost, D.J., Smyth, J.R., Laustsen, H.M.S., Kawamoto, T., Ross, N.L., and van Aken, P.A. (2004) Oxidation state of iron in hydrous mantle phases: implications for subduction and mantle oxygen fugacity. *Physics of The Earth and Planetary Interiors*, 143–144, 157–169. DOI:10.1016/j.pepi.2003.08.009
- Parise, J.B., Leinenweber, K., Weidner, D.J., Tan, K., and von Dreele, R.B. (1994) Pressure-induced H bonding: neutron diffraction study of brucite, $\text{Mg}(\text{OH})_2$, to 9.3 GPa. *American Mineralogist*, 79, 193–196.
- Smyth, J.R. (1994) A crystallographic model for hydrous wadsleyite ($\beta\text{-Mg}_2\text{SiO}_4$): An ocean in the Earth's interior? *American Mineralogist*, 79, 1021–1025.
- Smyth, J.R. and Kawamoto, T. (1997) Wadsleyite II: A new high pressure hydrous phase in the peridotite-H $_2$ O system. *Earth and Planetary Science Letters*, 146, E9–E16.
- Smyth, J.R., Holl, C.M., Frost, D.J., Jacobsen, S.D., Langenhorst, F., and McCammon, C.A. (2003) Structural systematics of hydrous ringwoodite and water in the Earth's interior. *American Mineralogist*, 88, 1402–1407.
- Smyth, J.R., Holl, C.M., Langenhorst, F., Laustsen, H.M., Rossman, G.R., Kleppe, A.K., McCammon, C.A., Kawamoto, T., and van Aken, P.A. (2005) Crystal chemistry of wadsleyite II and water in the Earth's interior. *Physics and Chemistry of Minerals*, 31, 691–705. DOI: 10.1007/s00269-004-0431-x

MANUSCRIPT RECEIVED AUGUST 15, 2005

MANUSCRIPT ACCEPTED MARCH 7, 2006

MANUSCRIPT HANDLED BY EUGEN LIBOWITZKY